JOURNAL OF SOLID STATE CHEMISTRY **140,** 285–294 (1998)
ARTICLE NO. SC987888

High-Resolution ^{19}F MAS and ^{19}F–^{113}Cd REDOR NMR Study of Oxygen/Fluorine Ordering in Oxyfluorides

Lin-Shu Du, Francis Wang, and Clare P. Grey[1]

Department of Chemistry, SUNY Stony Brook, Stony Brook, New York 11794–3400

Received November 14, 1997; in revised form May 13, 1998; accepted May 18, 1998

The ordering of fluoride ions on the anion sites in the oxyfluorides $Ba_2WO_3F_4$, $Ba_2MoO_3F_4$, $CdWO_3F_2$, $NaMoO_3F$, and K_2NbO_3F has been studied with very fast magic angle spinning ^{19}F NMR. ^{19}F MAS NMR of $Ba_2WO_3F_4$ shows that the fluoride ions are disordered within the four equatorial anion positions on the W–O/F chains, but that the anion positions between the chains are fully occupied by fluorine. No difference in fluoride-ion ordering is observed between samples synthesized under a wide variety of conditions (e.g., hydrothermally at 3 kbar at 800°C, and at 227°C at < 2 kbar.) In contrast, fluoride ions in the isostructural compound $Ba_2MoO_3F_4$ are almost completely ordered both between and on the W–O/F chains. Two-dimensional NMR is, however, used to demonstrate that a weak ^{19}F resonance corresponding to $\approx 0.35\%$ of the total fluoride-ion content is not due to a BaF_2 impurity but that it results from a small amount of disorder in the tungsten chains. The fluoride ions order on one site in $NaMoO_3F$ and K_2NbO_3F, consistent with earlier studies. The ^{19}F and ^{19}F–^{113}Cd REDOR NMR of $CdWO_3F_2$ show that the fluoride ions are ordered on two anion sites, each equidistant from a cadmium ion, in contrast to the isostructural compound $CuWO_3F_2$ where ordering on only one anion site has been proposed. A new model for the structure of $CdWO_3F_2$ is proposed. © 1998 Academic Press

INTRODUCTION

The problem of determining oxygen/fluorine ordering is unusual in that neither X-ray or neutron diffraction experiments can distinguish between oxygen and fluorine atoms. In many instances, where anion ordering has been proposed, this has been deduced from bond-strength bond-length calculations (1) or from Raman spectroscopy (2) and was not determined directly from the diffraction data. We have been using very fast ^{19}F MAS NMR to study O/F ordering in a series of tungsten and molybdenum oxyfluoride phosphor materials, systems in which a knowledge of anion ordering may lead to an improved understanding of their luminescent properties.

The results from the study of five different oxyfluorides are reported in this paper: $Ba_2WO_3F_4$, $Ba_2MoO_3F_4$, $CdWO_3F_2$, $NaMoO_3F$, and K_2NbO_3F. The structure of $Ba_2WO_3F_4$ (3, 4), and its isostructural compound $Ba_2MoO_3F_4$ (5), consists of chains of corner-sharing WO/F octahedra, which are separated by barium cations and two crystallographically distinct anion sites. Oxygen ordering on three out of the seven possible anion sites has been proposed, from bond-strength bond-length (BSBL) and Madelung lattice-energy calculations (4–6), to occur in $Ba_2WO_3F_4$: One oxygen atom bridges the tungsten atoms in the W–O–W chains, while the other two are ordered in a cis arrangement on the tungsten octahedra. This is shown in Fig. 1a. The extent of O/F ordering in $Ba_2MoO_3F_4$ is unknown. $CdWO_3F_2$ (7) is isostructural with the cuprate $CuWO_3F_2$ (8); its structure also consists of chains of trans-corner-sharing WO_4F_2 octahedra, which run parallel to the c axis. The octahedrally coordinated cadmium/copper atoms are located between the WO_4F_2 chains and form strings of edge-sharing octahedra (Fig. 1b). The single crystal study of the cuprate (8) revealed three O/F sites, and an O/F ordering scheme similar to that found in the barium tungstate was proposed from BSBL calculations: Again the $(WO_2F_2O_{2/2})_n^{2-}$ chains were formed from W–O–W linkages, the two remaining fluoride anions ordering in a cis-arrangement. A mirror plane through the tungsten octahedra results in only two crystallographically distinct equatorial anion positions on the tungsten octahedra: one of these sites is occupied by F and the other by O. The extent of O/F ordering in $CdWO_3F_2$ has not been determined. The structure of $NaMoO_3F$ (9) is built up of isolated chains of MoX_6 ($X = O, F$) edge-sharing octahedra with (octahedrally coordinated) sodium atoms occupying positions in between the chains. Fluorine atoms were proposed from BSBL, Raman, and Madelung-energy calculations to order in one of the four anionic sites ($X(3)$) (10). In addition, the second moment of the ^{19}F resonance obtained from ^{19}F wide-line NMR was consistent with either $X(3)$ ordering or

[1]To whom correspondence should be addressed. E-mail: cgrey@sbchem.sunysb.edu.

0022-4596/98 $25.00

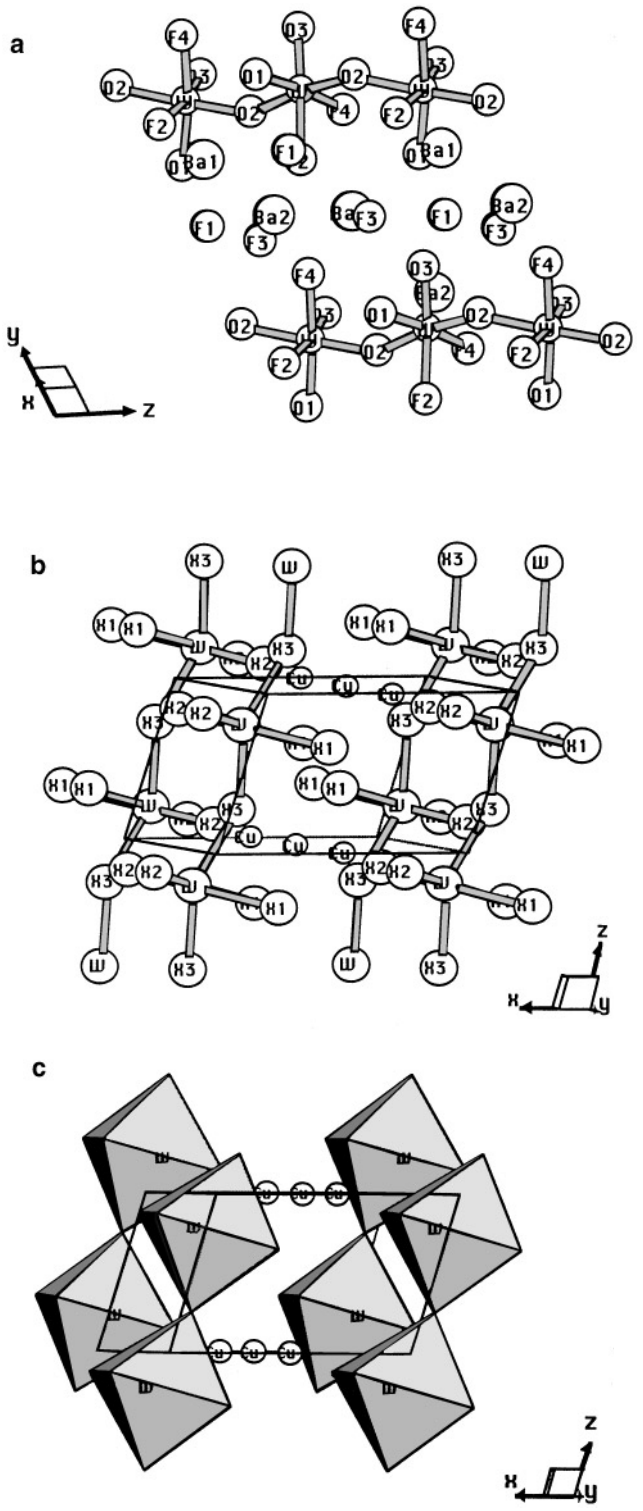

FIG. 1. The structures of some of the materials studied, or isostructural compounds, as determined from single crystal X-ray diffraction experiments. (a) A view of the $Ba_2WO_3F_4$ structure (4), drawn looking down the *x* axis to show the chains of tungsten octahedra. (b) A view down the *y* axis of the $CuWO_3F_2$ structure (8), showing the *X*1, *X*2, and *X*3 anion sites and (c) a polyhedral representation of the chains of tungsten octahedra in this compound.

a statistical distribution of F over all sites (10). The final compound studied, K_2NbO_3F (11), adopts the K_2NiF_4 structure (12), in which there are two crystallographically distinct anion sites. The anion site in the niobium planes is fully occupied by oxygen atoms, while the other anion site, above and below the Nb–O–Nb planes, is randomly occupied by oxygen and fluorine anions in a 1 : 1 ratio.

In this paper we demonstrate that one-dimensional ^{19}F NMR is extremely sensitive to small changes in local structure and ordering. Two-dimensional spin-diffusion methods (1, 13, 14) are used to determine whether any additional ^{19}F resonances that are observed are due to O/F disorder or whether they arise from the presence of impurity phases. Since spin diffusion involves the transfer of spin polarization (or magnetization) between nuclei in networks of dipolar-coupled spins, the observation of spin diffusion between two or more resonances indicates that the resonances arise from species within the same crystallite or phase (14). The two-dimensional spin-diffusion experiments can also be used to probe the local environment of the fluorine nuclei, since the dipolar coupling has a strong distance dependence (r^{-3}, where r is the internuclear distance). Given the limited number of high-resolution ^{19}F MAS NMR spectra of fluorides and oxyfluorides, assignment of the fluorine resonances is not always straightforward. We have, therefore, been exploring the sensitivity of these 2-D experiments to F–F proximity and whether these experiments can be used to aid in the assignment of the fluorine resonances.

The oxyfluorides chosen for study contain other NMR-active nuclei, and thus dipolar coupling to these nuclei may, in theory, be exploited to help spectral assignment and to gain additional structural information. Dipolar coupling between heteronuclei will be almost completely removed under the conditions of fast MAS used to acquire the ^{19}F spectra and, under slower MAS, will be obscured by the larger ^{19}F homonuclear coupling. The REDOR experiment of Gullion and Schaefer (15, 16) is, however, designed to reintroduce the dipolar coupling between specific sets of heteronuclei, allowing the dipolar coupling, and hence internuclear distances, between the heteronuclei to be measured. In this paper, the ^{19}F–^{113}Cd REDOR experiment is used to obtain Cd–F internuclear distances, which help determine the O/F ordering scheme in $CdWO_3F_2$.

EXPERIMENTAL

Sample preparation. Stoichiometric mixtures of the MF/MF_2 fluorides (M = Ba, Cd, K, Na) and M_2O_5/MO_3 oxides (M = Mo, W, Nb) were ground, pressed into 3 mm pellets, and placed into copper tubes which were crimped and sealed with silver solder. The tubes were heated for the following times and temperatures and were then slowly cooled to room temperature: $Ba_2WO_3F_4$, 5 days at 750°C; $Ba_2MoO_3F_4$, 5 days at 600°C; $NaMoO_3F$, 1 day at 460°C;

K_2NbO_3F, 1 day at 750°C; $CdWO_3F_2$, 1 day at 600°C. $Ba_2WO_3F_4$ and $Ba_2MoO_3F_4$ were also prepared by hydrothermal methods. The desired products were successfully obtained from a stoichiometric one gram mixture of BaF_2 and WO_3/MoO_3 in 15 ml of 3.2% HF solution. This mixture was placed in a Teflon-lined digestion container which was heated at 227°C for 3 days. $Ba_2WO_3F_4$ was also synthesized hydrothermally in an acidic fluoride solution, under 3 kbar of pressure, with a sealed gold tube inside a hydrothermal bomb. The temperature was maintained at 800°C for 3 days and was then slowly cooled to 300°C. A number of large single crystals were grown under these conditions and were ground for further characterization (diffraction and NMR). All samples were characterized with powder X-ray diffraction; X-ray powder patterns were compared to those reported in JCPDS or those simulated using the reported structures.

NMR. ^{19}F MAS NMR spectra were obtained with CMX-360 and CMX-200 spectrometers at operating frequencies for ^{19}F of 338.75 and 188.19 MHz, respectively. ^{19}F chemical shifts were referenced to a $CFCl_3$ solution, at 0 ppm, as an external reference. A Chemagnetics pencil probe with a reduced ^{19}F background signal was used. This probe is equipped with a high-speed MAS stator and 3.2 mm rotors that are capable of reaching spinning speeds of 24 kHz. Due to the small size of the rotors, only approximately 50 mg of sample was required. Typically, spectra were acquired with $\pi/2$ pulses of 2 μs, recycle delays of 10 s, each spectrum requiring approximately 100–500 acquisitions.

Two-dimensional spin-diffusion experiments were performed with a standard 2-D magnetization exchange pulse sequence (17):

$$\pi/2 - t_1 - \pi/2 - t_m - \pi/2 - \text{acquire } (t_2)$$

Spectra are required (in t_2), for successive time increments of the first time dimension (t_1). The magnetization is aligned with the static magnetic field during the mixing time of the 2-D sequence (t_m). Any spin-diffusion that occurs during this period is detected as a cross-peak in the 2-D spectrum after successive Fourier transformation along t_1 and t_2.

The ^{113}Cd MAS NMR was performed at an operating frequency for ^{113}Cd of 79.84 MHz with $\pi/2$ pulses of 3.0 μs and recycle delays of 10 s, at a field strength corresponding to 360 MHz proton frequency. Aqueous $Cd(ClO_4)_2$ at 0 ppm was used as an external reference. The ^{19}F–^{113}Cd REDOR experiments were performed with the fast MAS double resonance probe with $\pi/2$ pulses for ^{19}F of 2.0 μs. The following REDOR pulse sequence was used (15):

^{19}F: $\pi/2$ –τ– –τ– (–τ– –τ–)$_n$ π –τ– –τ– (–τ– –τ–)$_n$ – acquire

^{113}Cd: –τ– π –τ– (π –τ– π –τ–)$_n$ –τ– π –τ– (π –τ– π –τ–)$_n$

where the interval τ is given by half the rotor period (i.e., $1/2\nu_r$, where ν_r is the spinning speed). A string of $(2n + 1)$ ^{113}Cd π pulses is applied during the evolution and refocusing period of the ^{19}F spin echo experiment. The ^{19}F π pulse, applied after $n + 1$ rotor periods, serves to refocus the ^{19}F chemical shifts. One experiment is performed with the ^{113}Cd pulses, and the intensity of the ^{19}F resonance is measured (I). The experiment is repeated, without the ^{113}Cd pulses (the control experiment), in order to take into account any loss of ^{19}F intensity due to T_2 effects. The intensity measured in the control experiment (I_0) and in the REDOR experiment (I) are then measured as a function of n, the number of rotor periods of dephasing. A REDOR fraction $(1 - I/I_0)$ is then calculated for each value of n. Dipolar coupling constants, D, are extracted by simulating the REDOR dephasing curves (i.e., the REDOR fraction plotted as a function of dephasing time $(2(n + 1)/\nu_r)$) for specific values of D. The ^{113}Cd frequency was applied exactly on resonance, to minimize resonance offset effects. Experiments were performed with spinning speeds of 9, 15, and 18 kHz in order to explore the effect of ^{19}F spin diffusion on the REDOR dephasing curves. No significant differences were observed, and the results at fast spinning speeds are reported. In addition, the rate constants for spin diffusion between the two fluorine sites were determined from 2-D spin-diffusion experiments, performed with a variety of mixing times, analogous to those described earlier for $Ba_2MoO_3F_4$. Very small rate constants of 6 and 0.008 Hz, at spinning speeds of 10 and 20 kHz, respectively, were measured (18). These experimental data suggest that, at least at fast spinning speeds, the effect of ^{19}F–^{19}F homonuclear coupling on the REDOR curves may be ignored.

RESULTS

$Ba_2WO_3F_4$ and $Ba_2MoO_3F_4$ (1-D NMR). The ^{19}F MAS NMR spectra of $Ba_2WO_3F_4$ and $Ba_2MoO_3F_4$, prepared hydrothermally at 227°C, are shown in Fig. 2. Two groups of resonances are seen in both spectra, at approximately −20 and −100 ppm. Given the similarity in chemical shift between the higher frequency group of resonances and the ^{19}F resonance of BaF_2 (−14.2 ppm), these resonances are assigned to the fluorine atoms located in between the tungsten–O/F chains, that are coordinated to four Ba atoms (i.e., the F1 and F3 sites shown in Fig. 1a). The second group of resonances, is assigned to fluorine atoms coordinated to Mo/W atoms in the Mo/W chains. Since all the seven possible anion positions reported in the crystal structure of $Ba_2WO_3F_4$ (five coordinated to W and two between the W chains) are located on general positions (4*a* in space

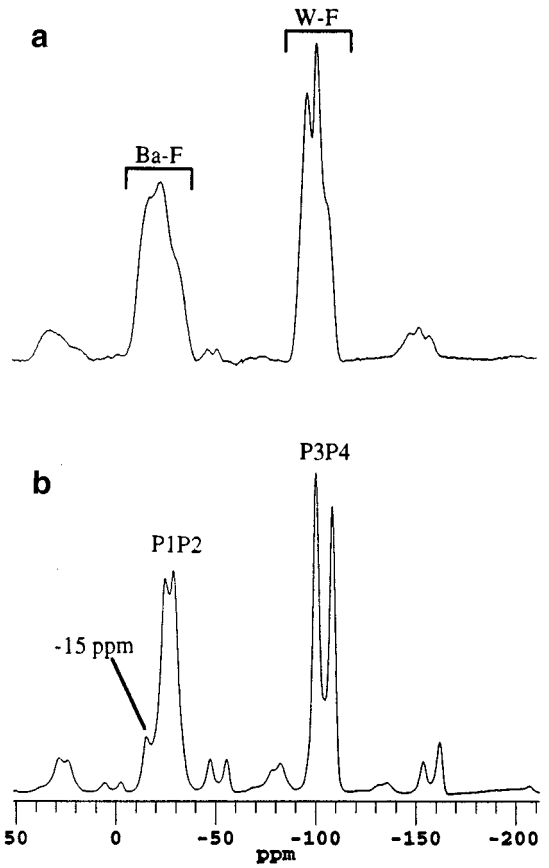

FIG. 2. ^{19}F MAS NMR spectra of (a) $Ba_2WO_3F_4$ and (b) $Ba_2MoO_3F_4$, collected at spinning speeds of 17 and 18 kHz, respectively, at a field strength corresponding to a 360 MHz proton frequency. The isotropic peaks are labeled "Ba–F" and "W–F" ($Ba_2WO_3F_4$), and P1–P4 and -15 ppm ($Ba_2MoO_3F_4$); the remaining peaks are spinning sidebands.

group *Cc*), four resonances of equal intensity are predicted if the anions are fully ordered. This is essentially the case for the spectrum of $Ba_2MoO_3F_4$ where two "barium fluoride" resonances at -24 and -28 ppm (labeled P1 and P2) and two "Mo–F" resonances at -100 and -108 ppm (labeled P3 and P4) are observed. In contrast, at least six major resonances are observed in the spectrum of $Ba_2WO_3F_4$ indicating that the anions in this material are disordered. Careful integration of the two sets of resonances (and associated spinning sidebands), (labeled "Ba–F" and "W–F" in Fig. 2a) gives a ratio of 1 : 1 for the relative intensities of the "Ba–F" and "W–F" sets of resonances. Assuming that there are no deviations from stoichiometry, this indicates that the anion sites in between the W–O/F chains and Mo–O/F are fully occupied by fluorine in both compounds. However, significant O/F disorder in the W/Mo chains occurs in $Ba_2WO_3F_4$.

Close inspection of the 1-D spectrum of $Ba_2MoO_3F_4$ reveals a small resonance at approximately -15 ppm, which accounts for approximately 0.35% of the total ^{19}F intensity. Given the similarity of this chemical shift to that of BaF_2 (-14.2 ppm), it is tempting to assign this to the presence of BaF_2 impurity; indeed in some preparations where BaF_2 was visible in the X-ray powder diffraction patterns, an increased intensity of this resonance was observed. However, this resonance was always observed even in samples where no BaF_2 could be detected in the powder diffraction patterns. The widths of the spinning sideband manifolds are of the same order of magnitude for all the resonances in the two compounds. However, small differences are noted. For example, that of P4 in $Ba_2MoO_3F_4$ is larger than that of P3.

There is little evidence for significant deviations from stoichiometry in the compound $Ba_2WO_3F_4$. Firstly, since fluorine-ion excess (resulting from the reduction of W(VI) to W(IV)), is more likely than fluorine-ion deficiency, off-stoichiometry should be seen as an increase in the concentration of "W–F" fluoride ions. Secondly, the compound is a white color consistent with the lack of W(IV) (19). Finally, the ^{19}F MAS NMR is not consistent with a significant concentration of paramagnetic ions (i.e., W(IV)) in the sample (20).

The single crystals of $BaWO_3F_4$ used in the earlier diffraction studies (4) were grown at higher temperatures and pressures than used in our initial syntheses. Thus, $Ba_2WO_3F_4$ was synthesized under conditions that very closely mimicked those used in the earlier syntheses, in order to explore the effect of sample preparation on the degree of fluorine ordering. No discernible differences could, however, be detected between the ^{19}F NMR spectra of the samples prepared by high-temperature calcination and by low- and high-temperature hydrothermal methods. We estimate the sensitivity to changes in site occupancy to be approximately 0.5–1%, based on S/N considerations and line widths of the resonances.

2-D NMR of $Ba_2MoO_3F_4$. In order to determine whether the resonance at -15 ppm results from BaF_2 or whether it results from a small degree of O/F disorder, we performed a series of 2-dimensional spin-diffusion experiments. Figure 3 shows the 2-D spectrum of $Ba_2MoO_3F_4$, acquired with a mixing time of 5 ms, and 1-D slices through the resonances at -15, -24 (P1), and -28 ppm (P2). The diagonal in the 2-D spectrum consists of two groups of two resonances, P1/P2 and P3/P4, and the small resonance at -15 ppm. Spin diffusion between two sets of spins will result in cross-peaks connecting the two resonances on the diagonal from these two spins. These cross-peaks can be seen more easily by taking slices through peaks. The slice of the resonance at -15 ppm (Fig. 3d) shows two major cross-peaks with P1 and P3; smaller cross-peaks with P2 and P4 are also observed. Cross-peaks with the resonance at -15 ppm are also observed in the slices through P3 and P4. It is clear that the resonance at -15 ppm results from ^{19}F nuclei in the same phase as the P1–P4 spins and thus does not belong to

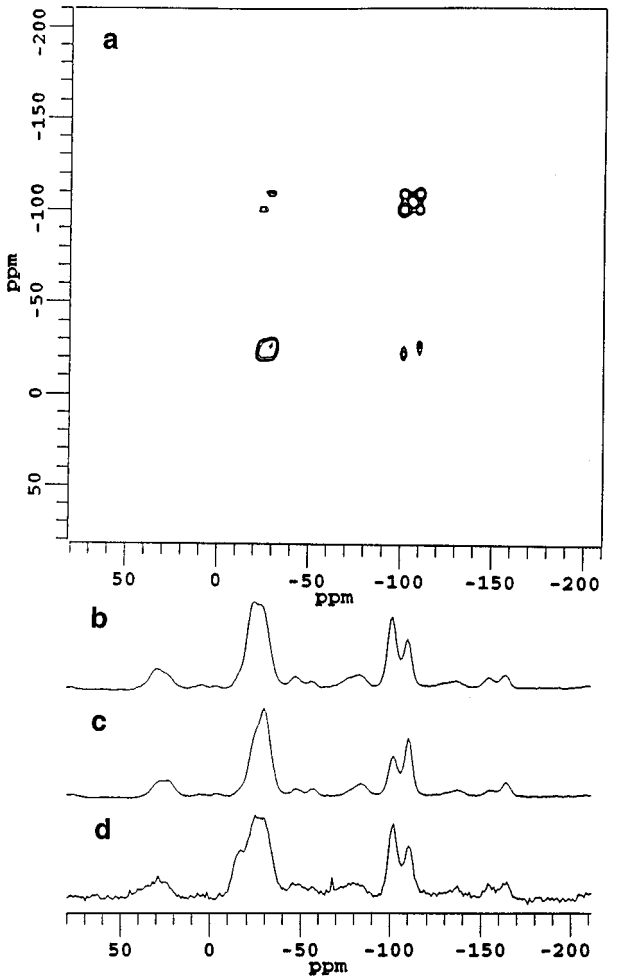

FIG. 3. (a) 2D ^{19}F exchange spectrum of $Ba_2MoO_3F_4$, collected at a spinning speed of 10 kHz with a mixing time of 5 ms, at a field strength corresponding to 200 MHz proton frequency. Horizontal slices of the 2D spectrum, through P1, P2, and the resonance at -15 ppm, are shown in (b), (c), and (d), respectively.

a BaF_2 impurity. P1 is connected to two intense cross-peaks from P2 and P3, and the P4 cross-peak is significantly smaller. In contrast, P2 is connected to P1 and P4, the cross-peak with P3 being less intense.

1-D Spectra of $NaMoO_3F$, K_2NbO_3F, and $CdWO_3F_2$. The fluorine atoms of $NaMoO_3F$ and K_2NbO_3F are predicted from BLBS and other calculations (10, 11) to be ordered on one anionic site. Their ^{19}F spectra are in accord with this (Fig. 4), single resonances being observed at -171 and -136 ppm, for the two compounds, respectively. Ordering on one anion site was also predicted for the isostructural compound of $CuWO_3F_2$, $CdWO_3F_2$. However, two distinct resonances are observed at -138 and -155 ppm in the ^{19}F spectrum of $CdWO_3F_2$, indicating that the fluorine ions are not located on a single anion position. In addition, the resonance at -155 ppm is associated with larger spinning

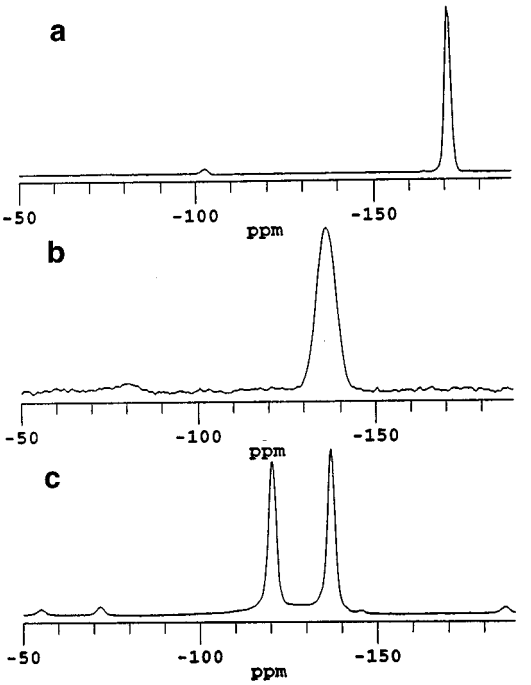

FIG. 4. ^{19}F MAS NMR spectra of (a) $NaMoO_3F$, (b) K_2NbO_3F, and (c) $Cd_2WO_3F_2$ collected at spinning speeds of 23, 19, and 22 kHz, respectively, at 360 MHz (^1H frequency).

sideband manifolds than the resonance at -138 ppm; this is more pronounced for spectra obtained at slower spinning speeds. Two-dimensional spin-diffusion shows cross-peaks between the two resonances, and thus these two resonances result from environments within the same crystallites.

Considerable variation in the ^{19}F line widths is observed for the three compounds. (Full-width at half-height line widths: 740, 2150, 860 (-138 ppm), and 800 Hz (-155 ppm) for $NaMoO_3F$, K_2NbO_3F, and the two resonances of $CdWO_3F_2$, respectively). The line width observed for $NaMoO_3F$ is less than those observed for $Ba_2MoO_3F_4$, for which line widths of 1130 (P3) and 1040 (P4) Hz were observed.

The ^{113}Cd ($I = \frac{1}{2}$) spectrum of $CdWO_3F_2$ shows a single sharp resonance at -173 ppm with a line width of 2.2 kHz at a spinning speed of 9.5 kHz. A single resonance, broadened by the second-order quadrupolar interaction, is seen in the ^{23}Na ($I = \frac{3}{2}$) MAS spectrum of $NaMoO_3F$. The resonance can be simulated by using a single set of values for the quadrupolar coupling constant (QCC), and asymmetry parameter of 1.6 MHz and 0.0, respectively, indicating that only one local environment for ^{23}Na is present.

^{19}F–^{113}Cd REDOR NMR. Experiments were performed as a function of the total number of rotor periods of dephasing (n), for both the control (no ^{113}Cd π pulses) and REDOR experiment. The REDOR fraction for both ^{19}F resonances was calculated from the intensities measured in the control

and REDOR experiments. The results are shown in Fig. 5. Both ^{19}F resonances show very similar dephasing curves, suggesting similar Cd–F internuclear distances. Both curves show a pronounced oscillation in the REDOR fraction, superimposed on a more steady increase. This behavior is observed in systems with more than one dipolar coupling (i.e., Cd–F internuclear distance) and most likely arises from the combination of large and some much smaller dipolar coupling constants. Note that the REDOR dephasing curves are a measure of the ^{113}Cd–^{19}F dipolar coupling only and are unaffected by the presence of ^{111}Cd: ^{111}Cd–^{19}F dipolar coupling could be measured in an analogous fashion, with a string of ^{111}Cd pulses.

The structure of $CuWO_3F_2$, and the Cu–F internuclear distances, were used as an approximate starting model for our simulations of the REDOR dephasing curves. The fluorine atom in this structure is coordinated to two Cu atoms with Cu–F distances of 1.96 and 2.53 Å. The next closest Cu atoms are more than 4 Å away. Thus, initial simulations were performed for each ^{19}F resonance by assuming that each F atom is coordinated to two Cd atoms in two nearby sites S_1 and S_2. The low natural abundance of the ^{113}Cd nucleus (12.26%) was taken into account as follows: the probabilities that the sites S_1 and S_2, which give rise to the dipolar couplings D_1 and D_2, respectively, are occupied by ^{113}Cd nuclei in the following arrangements were calculated and are ($0\,S_1$, $0\,S_2$) 0.7698; ($1\,S_1$, $0\,S_2$) 0.1076; ($0\,S_1$, $1\,S_2$) 0.1076; ($1\,S_1$, $1\,S_2$) 0.0150, where $1\,S_1$ indicates that the S_1 site is occupied by ^{113}Cd. Hence, the probability of two nearby ^{113}Cd nuclei is small and this local environment is ignored in the simulations. The large oscillations observed for both resonances were fit by manually varying the values of D_1 and D_2. The best fit was obtained when the same values were used for D_1 and D_2 (see Fig. 5), $D_1 = D_2 = 1.76$ kHz, giving two Cd–F internuclear distances of 2.4 Å. Thus we conclude that both fluorine atoms are equally close to two Cd atoms. This is very different from the $CuWO_3F_2$ structure. The fit to the REDOR curve is still poor at larger dephasing times, and clearly other more distant ^{113}Cd nuclei contribute to the dephasing. In the $CuWO_3F_2$ structure, the next nearest (non-bonded) Cu atoms are located at 4.09, 4.39, 4.42, and 5.32 Å. The curve can, however, be quite well fit at longer dephasing times by including a coupling to a further two nuclei with the same dipolar coupling constants of 290 Hz (4.4 Å), as shown in Fig. 5. Again, the less probable local environments where two, three or four of the nearby sites for cadmium are occupied by ^{113}Cd nuclei are ignored in the simulations. The simulations are sensitive to small changes D_1 and D_2, and a deviation of 0.1 Å results in a significantly poorer fit. This is demonstrated in Fig. 5, where the curves obtained for $D_1 = D_2 = 2.3$ and 2.5 Å are also shown. Thus an estimate for the error associated with the distance measurement is approximately $\pm$ 0.1 Å, and the distance measurements are obtained with reasonable precision. Given the number of assumptions made in the simulations, the accuracy of the distance measurement may not be so good. However, other REDOR experiments performed on a number of model compounds suggest that this error estimate is reasonable: for example, a ^{31}P–^{19}F distance of between 3.50 and 3.65 Å was determined from a ^{31}P-observed REDOR experiment on a sample of fluorinated calcium apatite ($Ca_5(PO_4)_3OH$) (21), in good agreement with the X-ray distance of 3.60 Å (22), despite the presence of additional fluoride ions located at 4.9 Å from the ^{31}P spins.

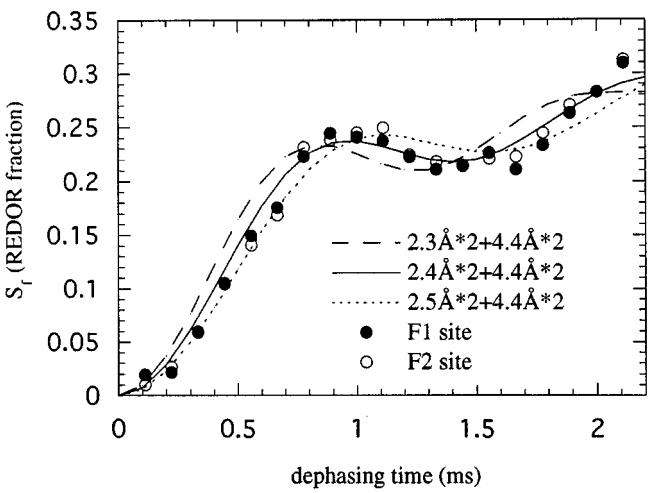

FIG. 5. The ^{19}F–^{113}Cd REDOR dephasing curves for $CdWO_3F_2$ were obtained at 360 MHz (^1H frequency) with a spinning speed of 18 kHz. The filled circles and open circles represent the measured data obtained for the resonances at -138 and -155 ppm, respectively. The solid line represents the calculated REDOR dephasing curves for two 2.4 and two 4.4 Å Cd–F internuclear distances; the dashed lines represent calculated curves where the two shorter Cd–F distances were varied by $\pm$0.1 Å.

DISCUSSION

$Ba_2WO_3F_4$ and $Ba_2MoO_3F_4$. The fluoride ions in the $Ba_2WO_3F_4$ structure are disordered among the anion sites, which is contrary to the ordering scheme proposed from BSBL calculations. The intensity ratios of the "Ba–F":"W–F" resonances indicates that there is full ordering of fluorine on the two anion sites between the layers. However, more than two fluorine resonances were observed in the "Ba–F" group, and the fluoride ions in the two anion sites between the chains appear to be affected by changes in O/F ordering that occur, locally, on the nearby tungstate chains. There are only two distinct groups of resonances. It is, therefore, extremely unlikely that any of the fluoride ions occupy the anion positions that bridge the tungsten atoms in the chains, since a fluorine atom in a W–F–W group is expected to resonate at a significantly different chemical shift position

than a fluoride atom bound to a single tungsten atom. Thus, the O/F disorder occurs in the four crystallographically distinct, equatorial anion positions of the tungsten octahedra, and is likely to occur due to differing arrangements of the two F and two O atoms. This could arise from different arrangements of *cis*-F–W–F groups from octahedron to octahedron, or from a combination of cis and trans-F–W–F arrangements. The dipolar coupling between fluorine atoms located in the cis and trans positions are very different (F–F distances of 2.7 (cis) and 3.8 Å (trans) corresponding to dipolar coupling constants of 8.1 and 2.9 kHz, respectively). The dipolar coupling between the fluorine atoms on and in between the chains is also significant, and cannot be ignored. For example, the F2 atom on the tungsten chains is only 3.06 Å from the nearest fluorine atom between the chains. Thus, the dipolar coupling is larger than that expected for two trans fluorine atoms. The spinning sidebands for all fluorine atoms on the tungsten chains are of the same order of magnitude, suggesting that the fluorine atoms are arranged in cis positions, but it is difficult to rule out trans arrangements completely without any additional information such as, for example, J couplings.

Despite the similarity of the Mo^{6+} and W^{6+} ionic radii, the anionic ordering in the two materials is very different, the ^{19}F NMR of $Ba_2MoO_3F_4$ showing almost complete ordering of the fluoride anions on four sites. The 2-D experiments, however, demonstrate that the small resonance at -15 ppm is due to fluoride ions in $Ba_2MoO_3F_4$ and is not an impurity. As was the case for $Ba_2WO_3F_4$, we cannot assign this resonance to another anion site located between the tungsten chains, since there are only two sites (F1 or F3). Thus this resonance is likely to be a result of small changes in the local environment around either F1 or F3, arising from O/F disorder in the tungstate chains. Furthermore, a large cross peak is seen in the 2-D spectrum of this material between this resonance and P3, while a much smaller cross-peak is seen with P4. Thus, a plausible explanation for the shift of the -15 ppm resonance, from the chemical shift position of either P1 or P2 (F1 or F3), is that a small fraction (0.35%) of the anion sites that gives rise to P4 are occupied by oxygen. The small fraction of fluoride ions that are displaced can then occupy either of the 2 oxygen positions on the tungsten chains. The new resonances that are generated most likely lie under P3 and P4 and are not clearly resolved, but may be responsible for the slight asymmetry in the resonances of P3 and P4. Further elucidation of the possible ordering schemes, however, requires that we assign the four major resonances (P1–4) to the four crystallographic sites for fluorine. We are currently using 2-D spin diffusion NMR methods to help assign these resonances further. Similar approaches have been used, for example, in the ^{13}C NMR of peptides and more recently in the ^{31}P NMR of inorganic phosphates, where connectivities have been observed with methods such as 2-D RFDR (23, 24). The situation here may be more complex, since there are typically many more coupled spins, and extended spin diffusion to more distant ^{19}F spins will occur for longer mixing times. Since spin diffusion rates depend on, not only the strength of the dipolar coupling between two or more spins, but also on the difference in chemical shifts of the resonances: a large separation in chemical shift between two resonances results in less effective overlap of the spectral density associated with the resonances, and consequently, less effective polarization transfer. This effect is expected to be more important for ^{19}F NMR than, for example, ^{1}H NMR, due to the large range of ^{19}F chemical shifts. Hence, larger cross-peaks are expected between resonances in the same group: i.e., between P1 and P2, and between P3 and P4. This was observed experimentally, and at shorter mixing times, the largest cross-peaks are observed between these resonances. Although the differences in cross-peak intensity between the groups of resonances will depend on differences in the dipolar couplings between the sets of coupled spins, many other factors are important such as the spinning speed, the size of the CSA and the relative orientations of the ^{19}F CSA tensors in the solid (14). We are currently exploring this further, and the results will be presented in a later paper.

$CdWO_3F_2$. The locations of the two different anion positions ($X1$(F) and $X2$(O)) [both 4*f* sites in space group $P2_1/m$] in the equatorial positions of the tungsten octahedra of the $CuWO_3F_2$ structure were shown in Fig. 1a. Two ^{19}F resonances of equal intensity were observed for $CdWO_3F_2$, indicating that the fluoride ions are located on two different anion sites and that the ordering scheme differs from that proposed for the cuprate.

A variety of different O/F ordering schemes can be envisaged. Occupation by fluorine of $X(3)$ i.e., the formation of W–F–W linkages is excluded, since a greater difference in chemical shifts between the two resonances than was observed experimentally is expected. The first possibility for ordering is that the fluoride ions are distributed over both the X_1 and X_2 sites, with a 50% occupancy of each site. This arrangement appears extremely unlikely, for a variety of reasons. Firstly, a single sharp resonance was observed in the ^{113}Cd spectrum of this compound, suggesting that the material is ordered. Secondly, the ^{19}F spectra of both $Ba_2MoO_3F_4$ and $Ba_2WO_3F_4$ have shown that ^{19}F is sensitive to differing arrangements of fluorine atoms, and different chemical shifts, or at least significant linebroadening, may be expected for each of the different possible fluoride-ion arrangements on the tungsten octahedra (i.e., for $2 \times X1$, $2 \times X2$, and $X1 + X2$). Another possible ordering scheme involves a reduction of space-group symmetry from $P2_1/m$ to $P2_1$. This is still consistent with the original indexing of the X-ray diffraction pattern (7). This reduction in symmetry involves the loss of the mirror plane that runs through the

tungsten atoms (in the xz plane). Four different anion sites are then generated in the unit cell, each with a multiplicity of 2, which we label $X1a$, $X1b$, $X2a$, and $X2b$, where $X1a$ and $X2a$ are cis fluoride ions. Six possibilities for ordering can be envisaged:

$X1a + X1b$, $X1a + X2a$, $X1b + X2b$, and $X2a + X2b$ (four configurations with *cis*-fluorines), and $X1a + X2b$ and $X1b + X2a$ (two configurations with *trans*-fluorines).

Each copper atom is coordinated to four $X1$ (fluoride) ions and two $X2$ (oxygen) ions in the $CuWO_3F_2$ structure. Each of the $X1$ fluorine atoms is then coordinated to two copper atoms (at 1.96 and 2.53 Å), so that the copper bridges two tungsten octahedra in the same chain (Fig. 1b). In contrast, $X2$ is coordinated to only one copper atom. The ^{113}Cd–^{19}F REDOR data for $CdWO_3F_2$ could be fit with a model in which both fluorine atoms are coordinated to two cadmium atoms 2.4 Å away. This is not consistent with fluorine ordering on either $X2a$ or $X2b$, where a dipolar coupling to only one nearby cadmium nucleus is expected. On this basis, ordering schemes involving both $X2a$ and $X2b$ are excluded and we are left with only one ordering scheme, $X1a + X1b$.

$CdWO_3F_2$ will differ from $CuWO_3F_2$ in that there will be no structural distortions due to the Jahn–Teller effect. The Jahn–Teller effect manifests itself in the two very different Cu–F distances (of 1.96 and 2.53 Å). (An even shorter Cu–O distance of 1.90 Å is also observed.) There are no electronic reasons to expect such differences in the Cd–F interatomic distances and this is consistent with our experimental findings from the REDOR NMR. A model for the structure of $CdWO_3F_2$, which takes into account the equidistant Cd–F bonds and is derived from small modifications of $CdWO_3F_2$ structure, can be obtained as described below.

Known unit cell parameters for $CdWO_3F_2$ ($a = 5.417$ Å, $b = 10.010$ Å, $c = 3.777$ Å, and $\beta = 105.652°$ (7)) and atomic positions for $CuWO_3F_2$ were used to simulate the $CdWO_3F_2$ structure. There are two sets of tungsten chains per unit cell (Fig. 1b) in $CuWO_3F_2$ where the tungsten atoms are located on the special position $[(x, \frac{1}{4}, z)$ and $(-x, \frac{3}{4}, -z)]$ and are related by a screw axis in the y direction at $(\frac{1}{2}\, y, \frac{1}{2})$. We propose that the tungsten chains in $CdWO_3F_2$ are translated in the z direction by a small amount c with respect to the chains in $CuWO_3F_2$. In order to preserve the screw axis, one chain (i.e., W, X_1, X_2, and X_3) must be translated by $+c$ and the second by $-c$, giving coordinates for the two tungsten atoms of $(x, \frac{1}{4}, z + c)$ and $(-x, \frac{3}{4}, -z - c)$ where c has been chosen so that the Cd atom lies directly between the $X1$ atoms forming an equilateral triangle. The enlarging the unit cell will result in an unrealistic lengthening in the W–X distances. Thus, the x and y coordinates for the $X1$ and $X2$ sites ($X1$ (0.3562, 0.3902), $X2$ (-0.1856, 0.1100)) were also modified by $\approx +0.008$ on $X1$ and -0.008 on $X2$ to ensure reasonable W–$X1$ and W–$X2$ distances of 2.0 Å, which are similar to those of $CuWO_3F_2$ (and also $Ba_2WO_3F_4$). If the W, $X1$, $X2$, and $X3$ atoms are then translated in the z direction by 0.0928 (i.e., $c = 0.0928$), then each of the Cd atoms will be equidistant between two $X1$ atoms (Fig. 6). Each $X1$ site will now have two Cd atoms at a distance of 2.36 Å in the first coordination shell and two Cd atoms at a distance of 4.34 Å in the second coordination cell. This is very close to the distances of 2.4 and 4.4 Å for the Cd atoms in the first and second coordination shells obtained from the experimental REDOR data. The Cd cations now have a much more symmetrical coordination environment with six fluorine atoms at 2.4 Å, consistent with the lack of a Jahn–Teller distortion for this compound. Powder X-ray diffraction structural studies of $CdWO_3F_2$ are currently in progress to confirm the NMR results, and to obtain accurate internuclear distances with which to simulate some of the NMR spectra.

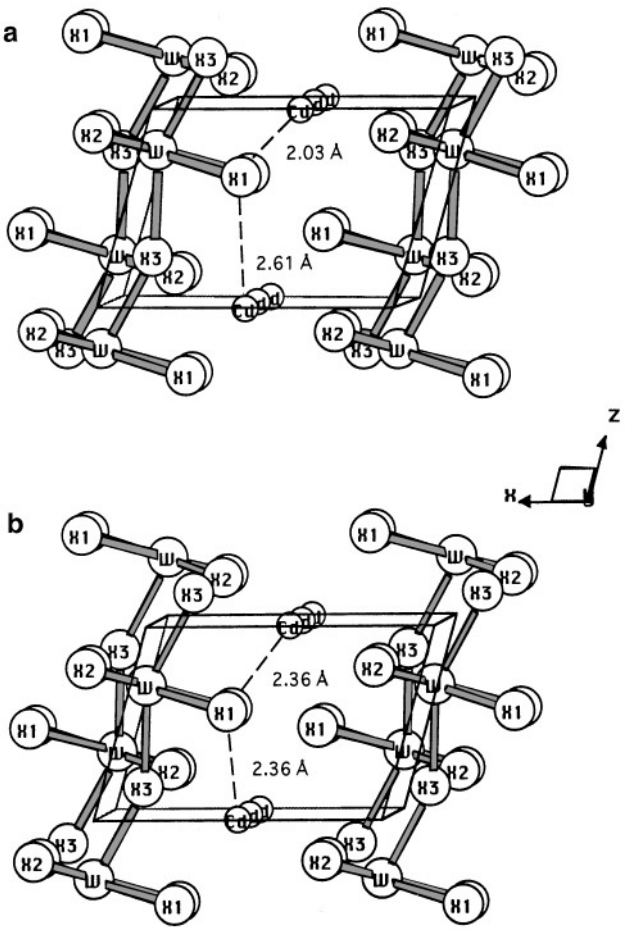

FIG. 6. A view down the y axis of the proposed $CdWO_3F_2$ structure showing how the new model was derived. (a) structure obtained from the cell parameters of $CdWO_3F_2$ and atomic positions of $CuWO_3F_2$. (b) Proposed model of $CdWO_3F_2$, in which each of the cadmium atoms is equidistant from two $X1$ atoms.

K_2NbO_3F. The fluoride ions of K_2NbO_3F are believed to be ordered on the 4*e* site of space group *I*4/*mm* (11), above and below the Nb–O–Nb planes. Anions on this site are coordinated to five K^+ and one Nb^{5+} cations. Only one broad resonance at -136 ppm is observed for K_2NbO_3F, close in frequency to the resonance of KF (-136 ppm), consistent with the proposed ordering scheme. The breadth of this resonance is likely a consequence of unresolved coupling to the quadrupolar nucleus ^{93}Nb and, possibly, of different ordering of fluorine atoms above and below the Nb–O–Nb planes. We have observed *J* coupling between ^{93}Nb and ^{19}F in K_2NbF_7 (25) consistent with the former suggestion.

Each Nb^{5+} ion in the K_2NbO_3F structure is coordinated to four oxygen anions in the Nb–O–Nb planes and two (O/F) anions sites above and below the planes. Two different methods for fluorine occupation of the sites above the planes can be envisaged: If the substitution is purely random, a distribution of NbO_6, NbO_5F, and NbO_4F_2 coordination environments will result. Alternatively, the fluorine anions could order in only one site per niobium octahedron, resulting in NbO_5F octahedra. The Nb–F bonds of the NbO_5F octahedra must, however, be randomly oriented above and below the plane with respect to each other, in order to maintain the apparent mirror plane located on the Nb–O–Nb planes, as observed by diffraction. Our results for $Ba_2WO_3F_4$ and $Ba_2MoO_3F_4$ showed that the ^{19}F chemical shifts are extremely sensitive to different ordering schemes of the O/F anions on the W/F octahedra. Thus, since we observe only one resonance for K_2NbO_3F, there do not appear to be a variety of very different local environments, and the NMR spectra suggest that each Nb^{5+} is coordinated to only one fluorine atom and exists as NbO_5F octahedron.

In general, the fluoride ions on the *M*O/F chains in all the compounds studied in this paper appear to be ordered on the anion sites that are also coordinated to the cations in between the chains. This is presumably due to the lower charge on the cations located between the chains, in comparison to the cations (Mo^{6+}, W^{6+}, Nb^{5+}) in the chains. The fluoride ion with its lower charge and its more ionic character, in comparison to the oxide anion, will occupy sites coordinated to the more ionic mono- and divalent cations. There was no evidence for ordering of fluoride ions in sites between the two W^{6+} or Mo^{6+} cations of the W/Mo chains, or in the Nb^{5+}–*X*–Nb^{5+} layers, and again this is most likely a consequence of the higher charge on these cations.

The ^{19}F chemical shifts of the different oxyfluorides follow some general trends. All these compounds can be written with a formula $N_nM_mO_xF_y$ (where *N* = Na, Ba, Cd and *M* = W, Mo, Nb), and consist of *M*O/F chains, *N* cations, and possibly extra fluoride ions, between the WO/F chains. The extra fluorine ions in between the chains are observed to resonate at frequencies close to the ^{19}F frequencies of the NF_2 or NF fluorides. For example, the fluoride ions between the W and Mo chains of $Ba_2WO_3F_4$ and $Ba_2MoO_3F_4$ resonate around -20 ppm, while the fluorine atoms in BaF_2 resonate at -14.2 ppm. The resonances of the fluorine atoms on the *M*O/F chains show a wide chemical shift range (-100 to -170 ppm) and depend on not only the nature of the *M* atom but also on the nature of *N*. The compounds, BaF_2, CdF_2, and NaF resonate at -14.2, -196, and -225 ppm, respectively, while the *M*–F fluorine ions in $Ba_2WO_3F_4$, $Ba_2MoO_3F_4$, $CdWO_3F_2$, and $NaMoO_3F$ resonate at approximately -100, -100, -150, and -170 ppm, respectively. Thus, each of the *M*–F ^{19}F resonances appears to be shifted from a hypothetical *M*–F chemical shift position of approximately -130 ppm, in the direction of the chemical shift of the mono/divalent fluorides.

CONCLUSIONS

Very fast 1- and 2-D ^{19}F MAS NMR spectra of a number of oxyfluoride materials demonstrate the sensitivity of ^{19}F NMR to small changes in anion ordering. Small amounts of disorder of less than 1% can be detected directly, amounts that would be very difficult to detect by other methods, including wideline NMR, or to predict from indirect methods such as bond length-bond strength calculations. Individual crystallographic fluorine sites can be resolved at spinning speeds as low as 10 kHz in these materials, and small changes in fluorine local environments even in the second coordination sphere (i.e., first anion coordination sphere) can result in significant changes in ^{19}F chemical shifts. Our results obtained for $Ba_2WO_3F_4$ demonstrate that indirect methods for the determination of oxygen/fluorine ordering such as bond-length bond-strength calculations or Madelung calculations may not always be correct. Two-dimensional NMR methods based upon spin diffusion between dipolar coupled fluorines were shown to be a simple and convenient method for determining whether fluorine resonances arise from fluorine atoms in the sample phase or whether they are present in impurity phases. This is of particular importance when studying fluorides where very low concentrations of impurities (and/or disorder) can be detected.

Heteronuclear dipolar recoupling sequences such as REDOR NMR can provide complementary structural information, as was shown in the case of $CdWO_3F_2$. The Cd–F internuclear distances obtained from this method were used to construct a new model for the structure of $CdWO_3F_2$. The model was based on the $CuWO_3F_2$ structure, but involved translations of the tungsten chains in the *z* direction to create a more symmetrical coordination environment for cadmium, in comparison to that of copper in $CuWO_3F_2$.

In conclusion, we have shown that very fast ^{19}F MAS NMR provides a simple method for directly probing anion ordering in oxyfluoride materials. We are currently extending these techniques to study a variety of oxyfluoride phosphors such as LiW_3O_9F, $Na_5W_3O_9F_5$, and $Pb_3W_2O_6F_6$ and are applying new homonuclear dipolar recoupling sequences to help assign the resonances and extract further structural information.

ACKNOWLEDGMENTS

We thank C. C. Torardi for synthesizing $Ba_2WO_3F_4$ hydrothermally (at 800°C) and for many helpful comments. This research was supported by the National Science Foundation through the NYI Program (DMR 9458017) and through a grant to purchase the NMR spectrometer (CHE-9405436). Additional support from the Alcoa Foundation through a Science Support Grant is gratefully acknowledged.

REFERENCES

1. D. Suter and R. R. Ernst, *Phys. Rev. B* **32,** 5608 (1985).
2. I. R. Beattie and T. R. Gilson, *J. Chem. Soc.* (*A*) 2322 (1969).
3. V. R. Domesle and R. Hoppe, *Z. Anorg. Allg. Chem.* **492,** 63 (1982).
4. C. C. Torardi and L. H. Brixner, *Mater. Res. Bull.* **20,** 137 (1985).
5. G. Wingefeld and R. Hoppe, *Z. Anorg. Allg. Chem.* **518,** 149 (1984).
6. I. D. Brown and R. D. Shannon, *Acta Crystallogr., Sect. A* **29,** 266 (1973).
7. J. P. Chaminade, A. Garcia, F. Guillen, and C. Fouassier, *Mater. Sci. Eng. B* **6,** 5 (1990).
8. J. M. Moutou, H. P. Francisco, J. P. Chaminade, M. Pouchard, and P. Hagenmuller, Z. *Anorg. Allg. Chem.* **539,** 165 (1986).
9. J. M. Moutou, J. P. Chaminade, M. Pouchard, and P. Hagenmuller, *Rev. Chim. Mineral.* **23,** 27 (1986).
10. J.P. Chaminade, J. M. Moutou, G. Villeneuve, M. Couzi, M. Pouchard, and P. Hagenmuller, *J. Solid State Chem.* **65,** 27 (1986).
11. F. Galasso and W. Darby, *J. Phys. Chem.* **66,** 1318 (1962).
12. D. Baltz and K. Plieth, *Z. Elektrochem.* **59,** 545 (1955).
13. C. E. Bronniman, N. M. Szeverenyl, and G. E. Maciel, *J. Chem. Phys.* **79,** 3694 (1983). W. A. Maas, Ph.D. Thesis, University of Nijmegen, 1992 [p. 19].
14. L. B. Moran, J. K. Berkowitz, and J. P. Yesinowski, *Phys. Rev. B* **45,** 5347 (1992).
15. T. Gullion and J. Schaefer, *J. Magn. Reson.* **81,** 196 (1989).
16. T. Gullion and J. Schaefer, *Adv. Magn. Reson.* **13,** 55 (1989).
17. J. Jeener, B. H. Meier, P. Bachmann, and R. R. Ernst, *J. Chem. Phys.* **71,** 4546 (1979).
18. L. S. Du and C. P. Grey, in preparation.
19. A. W. Sleight, *Inorg. Chem.* **8,** 1764 (1969).
20. C. P. Grey, Ph.D Thesis, Oxford Uiversity, 1991.
21. Y. Pan, *Solid State NMR* **5,** 263 (1995).
22. R. Z. LeGeros, *in* "Monographs in Oral Science" (H. M. Myers, Ed), Vol. 15, p. 4, Karger, New York, 1991.
23. A. E. Bennett, J. H. Ok, and R. G. Griffin, *J. Chem. Phys.* **96,** 8624 (1992).
24. C. Jager, M. Feike, R. Born, and H. W. Spiess, *J. Non-Cryst. Solids* **180,** 91 (1994).
25. F. Wang and C. P. Grey, unpublished results.